Numerical simulation of the seasonal precipitation amount over the Himalayan mountain region using the JMA-NHM

Akihiro Hashimoto[1], Masashi Niwano[1], Hatsuki Fujinami[2], Akiko Sakai[3], and Koji Fujita[3]

[1]*Meteorological Research Institute, Japan Meteorological Agency, Tsukuba, Japan*
[2] *Institute for Space-Earth Environmental Research, Nagoya University, Nagoya, Japan*
[3]*Graduate School of Environmental Studies, Nagoya University, Nagoya, Japan*

1. Introduction

In the last several decades, there has been a rapid retreat of the Himalayan glaciers. This has raised concerns regarding the effect of glacial retreat on river flow and water resources in South Asia which is experiencing rapid population growth. Precipitation over the Himalayan mountain region is a strong factor that affects the mass balance of the glaciers. For reliable prediction of the mass retreat of glaciers, it is necessary to understand the spatiotemporal distribution of precipitation and its impact on glacier mass balance and dynamics of water discharge. Satellite earth observation projects, such as Tropical Rainfall Measuring Mission (TRMM) and Global Precipitation Measurement (GPM), provide valuable data that enable statistical evaluation of the spatial distribution of precipitation covering a broad area, including the Himalayas. However, it is difficult to apply such data for detailed evaluation of seasonal changes to precipitation quantity and patterns due to intermittent spaceborne measurements. A complementary solution to address this issue is to use a numerical weather prediction (NWP) model. In this study, we plan to evaluate the glacier accumulation in the Himalayan mountain region using an NWP model with fine grid spacing. This report presents the results of preliminary simulations in terms of the sensitivity of simulated precipitation to grid spacing.

2. Numerical prediction system

The numerical prediction system was established based on the Japan Meteorological Agency's Non-Hydrostatic Model (JMA-NHM; Saito et al., 2006). The model was configured in the same manner as that previously used for the operational weather forecast in Japan, with the exception of the following: (i) in this study, a double-moment bulk parameterization scheme, predicting the mixing ratio and number concentration, was applied to all the three types of solid hydrometeors (cloud ice, snow and graupel), whereas this scheme was applied only to cloud ice in the original configuration; (ii) the ice-saturation adjustment scheme (Tao et al., 1989) was switched off to avoid the unrealistic formation of ice clouds in the upper troposphere.

Numerical predictions were conducted once a day from 1 June, 2018, to 31 May, 2019. For each prediction, the simulation was first conducted with a 5-km horizontal resolution (5km-NHM). The computational domain spans 2000 km × 2000 km wide (Fig. 1). Next, a convection permitting simulation with a 1 km horizontal resolution (1km-NHM) was conducted without cumulus parameterization in the domain (800 × 800 grid cells) embedded within the 5km-NHM (Fig. 1). Both domains were centered at Kathmandu, Nepal. The Lambert conformal conic projection was adopted, using 30.00 and 60.00°N for the

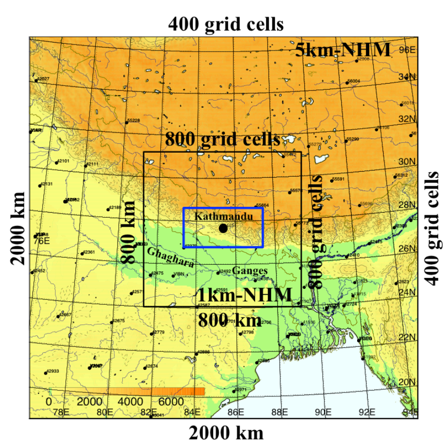

Fig. 1. Computational domains for weather prediction simulations with the 5km- and 1km-NHMs. The blue box shows the sampling area analyzed for seasonal changes in altitudinal variations of accumulated precipitation.

Corresponding author: Akihiro Hashimoto, Meteorological Research Institute, 1-1 Nagamine, Tsukuba, 305-0052, Japan. E-mail: ahashimo@mri-jma.go.jp

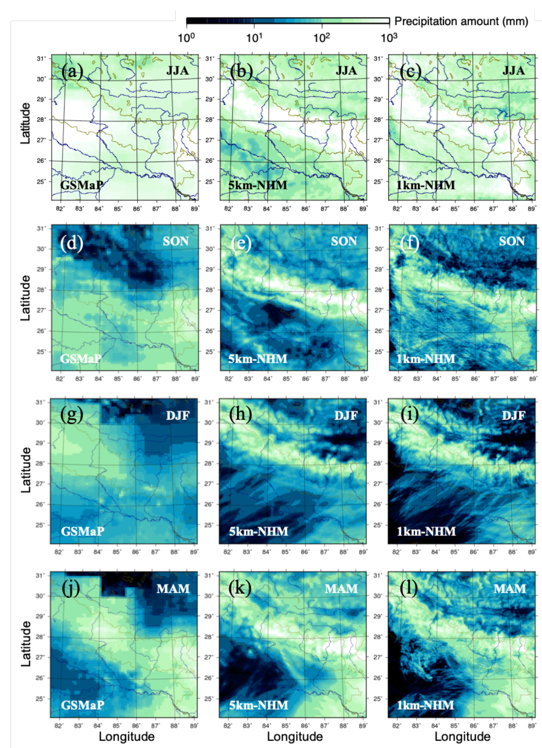

Fig. 2. Distributions of seasonal accumulated precipitation amount within the area corresponding to the domain of the 1km-NHM based on the observations with GSMaP (a, d, g, j), and the simulations with the 5km-NHM (b, e, h, k) and 1km-NHM (c, f, i, l). JJA, SON, DJF, and MAM indicate three-month periods from June, September, December 2018, and March 2019, respectively.

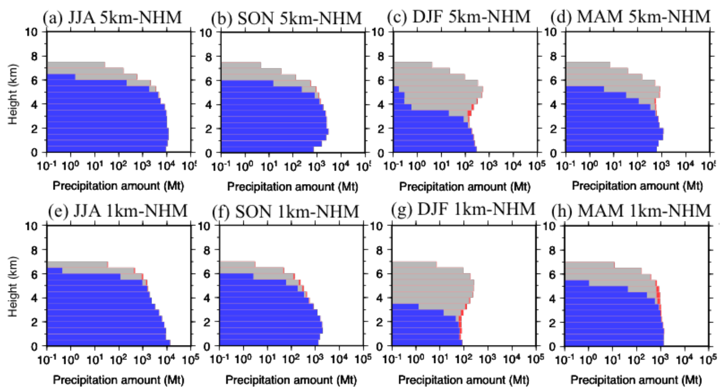

Fig. 3. Altitudinal variations of the three-month accumulated precipitation amount in the (a, e) JJA, (b, f) SON, (c, g) DJF, and (d, h) MAM periods from the simulations using the 5km-NHM (a, b, c, d) and 1km-NHM (e, f, g, h). Blue, grey, and red indicate different precipitation types: rain, snow, and graupel, respectively. The height interval is 500 m.

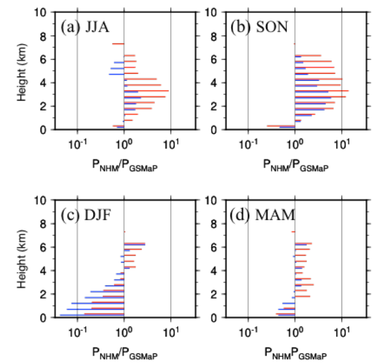

Fig. 4. Altitudinal variations of the ratio of the accumulated precipitation amount from simulations to the accumulated precipitation from GSMaP. The red and blue bars show the results generated by the 5km- and 1km-NHMs, respectively.

first and second standard latitudes, respectively, and 85.00°E for the standard longitude in both domains. The top height of the domain was 22 km, and there were 50 layers in the vertical direction, increasing from 40 m thick at the surface to 886 m at the top based on a terrain-following coordinate system.

The integration time for the 5km-NHM was 48 h, with a timestep of 8 s. The initial and boundary conditions were obtained from the JMA's operational global forecast. The simulation commenced at 1200 coordinated universal time (UTC), corresponding to a forecast time (FT) of 6 h in the JMA's operational global forecast beginning at 0600 UTC. The boundary conditions were provided every 6 h. For the 1km-NHM, the simulation commenced at a FT of 18 h in the 5km-NHM simulation, and the integration time was 27 h with an 8 s timestep. The initial and boundary conditions were obtained from the 5km-NHM.

3. Simulation results

Figure 2 illustrates the distributions of seasonal accumulated precipitation amount provided by the Global Satellite Mapping of Precipitation (GSMaP), and that simulated using the 5km- and 1km-NHMs. Whilst the GSMaP product has a bias compared to rain gauge measurements, in the present context, we considered it representative of observed data for comparison with the simulation results in this report. In summer (June-August; JJA), the GSMaP shows that the precipitation area covers the low land surrounding the Ghaghara and Ganges rivers, the high altitude mountain area, and the Tibetan plateau (Fig. 2a). The 5km-NHM underestimated the precipitation in the low land area (Fig. 2b), whilst the 1km-NHM provided a better prediction of this distribution in the low land area. (Fig. 2c). The precipitation decreases in autumn (September-November; SON), particularly in the Tibetan plateau (Fig. 2d). The 5km-NHM showed negative bias toward the low land area, and a positive bias toward the high mountain area and Tibetan plateau (Fig. 2e), compared with GSMaP. The 1km-NHM predicted greater precipitation in the low land than in the Tibetan plateau (Fig. 2f), consistent with results from GSMaP (Fig. 2d). Although precipitation in the high mountain area was overestimated, the 1km-NHM generally provided more accurate results than the 5km-NHM. However, the superiority of the 1km-NHM over the 5km-NHM was unclear in winter (December–February; DJF) and spring (March–May; MAM).

Figures 3 shows the altitudinal variations of precipitation amount within the blue box in Fig. 1 for different seasons simulated with the 5km- and 1km-NHM. In summer (JJA) and autumn (SON), the 1km-NHM predicted greater precipitation in the low land area at altitudes less than 500 m (Figs. 3e and 3f), compared with the 5km-NHM (Figs. 3a and 3b). Beyond 2 km above sea level (a.s.l.), the predicted precipitation by the 1km-NHM was less than predicted by the 5km-NHM. These features are consistent with the results in Fig. 2, where there is greater and reduced precipitation in low and high land areas, respectively, in the 1km-NHM than in the 5km-NHM. Figure 4 presents the ratio of the accumulated precipitation amount from the 5km-NHM (red bar) or 1km-NHM (blue bar) simulations to the GSMaP. The results of the 1km-NHM show better agreement with GSMaP than the results from the 5km-NHM in summer and autumn (Figs. 4a and 4b, respectively). This is consistent with the features presented in Fig. 3. In winter (Fig. 4c), the 1km-NHM underestimates precipitation at altitudes lower than 3 km. In spring (Fig. 4d), the 1km-NHM showed better results at the altitudes higher than 2 km.

The simulation results demonstrate the effectiveness of adopting a 1 km convection permitting grid spacing for regional simulation of precipitation in the Himalayan mountain region, particularly, for summer and autumn. However, rain-gauge-based validation is necessary to ensure the improved performance of the 1 km grid spacing.

Acknowledgements

This study is partly supported by the Joint Research Program with Swiss National Science Foundation "High elevation precipitation in High Mountain Asia" of Japan Society for the Promotion of Science (JPSP), and the Ministry of the Environment of Japan through the Experimental Research Fund for Global Environmental Research Coordination System.

References

Saito, K., T. Fujita, Y. Yamada, J. Ishida, Y. Kumagai, K. Aranami, S. Ohmori, R. Nagasawa, S. Kumagai, C. Muroi, T. Kato, H. Eito, and Y. Yamazaki, 2006: The operational JMA nonhydrostatic mesoscale model. *Mon. Wea. Rev.*, **134**, 1266–1298.

Tao, W.-K., J. Simpson, and M. McCumber, 1989: An ice- water saturation adjustment. *Mon. Wea. Rev.*, **117**, 231–235.